Title
Structural studies of the T∗-phases (La, Tb, Pb)2CuO4, (La, Tb, Sr)2CuO4 Structural transition in (La, Tb, Pb)2CuO4

Journal
Physica C Superconductivity, 171(5-6)

ISSN
0921-4534

Authors
Bordet, P
Cheong, S-W
Fisk, Z
et al.

Publication Date
1990-11-01

DOI
10.1016/0921-4534(90)90260-l

Physica C 171 (1990) 468–478
North-Holland

Structural studies of the T*-phases $(La, Tb, Pb)_2CuO_4$, $(La, Tb, Sr)_2CuO_4$

Structural transition in $(La, Tb, Pb)_2CuO_4$

P. Bordet [a], S-W. Cheong [b,c], Z. Fisk [c], Th. Fournier [a], J.L. Hodeau [a], M. Marezio [a,b], A. Santoro [d] and A. Varela [a]

[a] *Laboratoire de Cristallographie CNRS-UJF, 166X, 38042 Grenoble cedex, France*
[b] *AT&T Bell Laboratories, Murray Hill, NJ 07974, USA*
[c] *Los Alamos National Laboratory, Los Alamos, NM 87545, USA*
[d] *National Institute of Standards and Technology, Gaithersburg, MD 20899, USA*

Received 19 July 1990

The structure of the T* phase compound $(La, Tb, Pb)_2CuO_4$ has been investigated by single crystal X-ray diffraction as a function of temperature. It is shown that a structural transition exists around ≈ 470 K below which the structure is orthorhombic with cell parameters $a=b=5.451(2)$ Å and $c=12.462$ Å at room temperature. Annealing at temperatures above the transition favors the long range ordering of the superstructure. The tetragonal structure of the high temperature phase (space group P4/nmm) is similar to that determined by Izumi et al. [3] for the $(Nd, Sr, Ce)_2CuO_4$ T*-compound. This is also the case for the structure of $(La, Tb, Sr)_2CuO_4$ determined at room temperature by refinement of neutron powder diffraction data. The comparison of the three structures indicates that the disorder of the O(2) apical oxygen atoms is due to a dynamically disordered canting of the CuO_5 pyramids rather than to cation ordering on the 9-coordinated site. The structural transition is due to the ordering of this canting and is believed to be a general feature of the T*-phase compounds.

1. Introduction

The 2:1:4 cuprate superconductors are known to crystallize with three structures, the K_2NiF_4-type, the Nd_2CuO_4-type and the more recently discovered $(Nd, Sr, Ce)_2CuO_4$-type [1]. For brevity they will be referred to as the T, T′ and T* phases, respectively. These structures can be easily distinguished if they are described as built of (AO) and (BO_2) layers arranged as to form either ABO_3 perovskite or NaCl blocks. The three structures have the following sequences:

T		T*		T′
	$(BO_2)_o$		$(BO_2)_o$	$(BO_2)_o$
	$(AO)_c$		$(AO)_c$	$(A')_c$
	$(AO)_o$		$(AO)_o$	$(O_2)_o$
	$(BO_2)_c$		$(BO_2)_c$	$(A')_o$
	$(AO)_o$		$(A')_o$	$(BO_2)_c$
	$(AO)_c$		$(O_2)_o$	$(A')_o$
	$(BO_2)_o$		$(A')_c$	$(O_2)_o$
			$(BO_2)_o$	$(A')_c$
				$(BO_2)_o$

The o and c subscripts indicate whether the cations are at the origin or at the center of the mesh. In the (A′) layers all the oxygen atoms have been removed while in the (O_2) layers all the cations are absent. In this latter case the subscripts refer to cation empty sites. In the T structure the A cations are surrounded by 9 oxygen neighbors forming cuboctahedra in which the top four or bottom four anions have been replaced by one. The B cations are sur-

rounded by apically elongated octahedra. In the T′ structure the A′ cations are surrounded by 8 oxygen atoms arranged as a square prism, while the B cations are surrounded by four oxygen atoms arranged as a square. Since these squares are the remnants of octahedra, they form cornersharing layers.

In the T* structure the sequence of (AO) and (BO_2) layers is such that it comprises alternately one half the T′ unit cell and one half the T unit cell. There are two sites for the large cations, one 9-coordinated A inside the T/2 cell, and one 8-coordinated A′ inside the T′/2 cell. Since the (BO_2) layers are always sandwiched between an (AO) layer and an (A′) one, the B cations are surrounded by square pyramids forming corner-sharing pyramidal layers. These layers are one of the common features for most of the cuprate high-T_c superconductors.

As pointed out by Takayama-Muromachi et al. [1] all the cations and the oxygen atoms of the (CuO_2) layers occupy, besides local distortions, the same positions in the three structures, T, T′ and T*. The main difference between the three structures lies in the positions of the oxygen atoms of the large cation layers.

The compound (Nd, Sr, Ce)$_2$CuO$_{4-y}$ having the T* structure was reported to become superconducting by Akimitsu et al. [2]. The structural arrangement of the T* phase was determined by the combined use of X-ray and neutron powder diffraction, and high resolution electron microscopy [1]. It was found to be tetragonal, space group P4/nmm with lattice parameters, $a \approx 3.86$ Å and $c \approx 12.5$ Å. From neutron powder data, Izumi et al. [3] refined the structure of a $Nd_{1.32}Sr_{0.41}Ce_{0.27}CuO_{4-y}$ sample which had been fully oxidized and found to become superconducting. These authors carried out as well the structural refinement of a deoxidized, nonsuperconducting sample. However, no appreciable differences were found between the two structures. The 9-coordinated A sites were found to be occupied by 59% of Nd and 41% of Sr, while the 8-coordinated A′ sites were occupied by the remainder of the Nd cations and the Ce ones. From the interatomic distances and the site preferences Izumi et al. argued that the Ce atoms were likely in the 4^+ state, which was confirmed by XPS data. The O(2) atoms of the ((Nd, Sr)O) layers which are apexes of the CuO_5 pyramids had a large thermal factor indicating disordered static displacements attributed to partial ordering of the Nd^{3+} and Sr^{2+} cations on the A sites. The occupancy factor of the same O(2) atoms was found to be 0.92 for both the fully oxidized and the deoxidized samples, which corresponds to a formal valence of 1.98 for the Cu cations. To justify the superconducting properties of the oxidized sample the authors suggested that the samples have inhomogeneous domain structures in which oxygen-rich superconducting regions coexist with oxygen-poor nonsuperconducting regions.

We have carried out structural studies of two compounds which exhibit the T* structure. (La, Tb, Sr)$_2$CuO$_4$ has been investigated by neutron powder diffraction and found to be tetragonal at room temperature, like (Nd, Sr, Ce)$_2$CuO$_4$. However, single crystal X-ray diffraction study on (La, Tb, Pb)$_2$CuO$_4$ shows an orthorhombic structure at room temperature. At about 470 K this compound undergoes a phase transition where its symmetry becomes tetragonal.

2: Sample preparation

Single crystals of $La_{2-x}Tb_xCuO_4$ were grown from a CuO/PbO flux. La_2O_3, Tb_4O_7, CuO and PbO powders were mixed in the weight ratio of 1.29:0.71:4:2.8. This mixture was heated to 1250°C for 4 h, slowly cooled to 800°C during a period of 100 h and then furnace-cooled to room temperature. Small single crystal platelets, ($\approx 0.5 \times 0.5 \times 0.1$ mm^3) were removed mechanically from the flux. They were examined by energy dispersive microanalysis using a JEOL 840A SEM and a Kevex delta class system. The presence of a small quantity of lead coming from the flux was detected in all of them. The single crystal used in the X-ray diffraction data collection yielded the following composition:

$$(La_{0.565}Tb_{0.405}Pb_{0.030})_2Cu_{1.00}O_x\,.$$

The polycrystalline sample of nominal composition (La_1 $Tb_{0.8}$ $Sr_{0.2}$)CuO_4 was prepared by firing powders of the metal oxides and strontium carbonate at 950°C for 12 h, with one regrinding. These samples were then reground, pelletized and fired at 1000°C for 12 h, and reground again, pelletized and

fired at 1100°C for 12 h. All firings were done in air, and the sample was furnace-cooled.

3. Symmetry and structure of (La, Tb, Pb)$_2$CuO$_4$

3.1. Precession camera studies

The single crystal platelets were characterized by X-ray diffraction using a precession camera and Zr filtered MoKα radiation. All reflections corresponded to the P4/nmm space group of the T* phase with cell parameters $a_p = b_p \approx 3.86$ Å and $c \approx 12.46$ Å. However, longer exposures of the ($hk0$) and ($hk1$) reciprocal planes revealed the presence of weak superstructure spots which could not be indexed on the above cell but were indexable on the diagonal unit cell $a_p\sqrt{2} \times a_p\sqrt{2} \times c$ (see fig. 1). With this cell, the systematic absences among the ($hk0$) reflections occur when h and k are both odd. Such an extinction rule does not correspond to any translation symmetry element. It can be explained by assuming that the extra spots occur only along one direction, that the crystal is twinned by the (110) plane and that the symmetry is orthorhombic. The observed (hkl) reflections contain the intensity of the (hkl) reflection of the I twin individual plus the intensity of the (khl) reflection of the II twin individual. In the ($hk0$) plane, the reflections with h and k even follow this rule, while those with h and k of different parity contain the contribution from only one domain. No reflection splitting due to twinning was observed on the precession photographs. The same superstructure pattern was observed for all crystals tested.

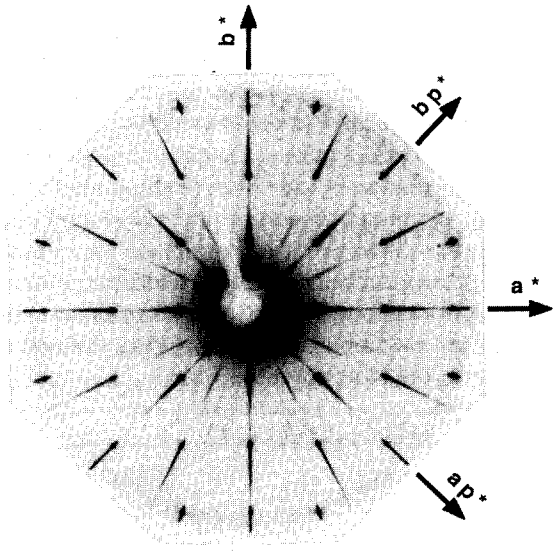

Fig. 1. Precession camera photograph showing the ($hk0$) reciprocal plane of a (La, Tb, Pb)$_2$CuO$_4$ single crystal at room temperature. The superstructure spots are clearly visible.

In order to determine the behavior of the superstructure with temperature, the precession photographs containing the extra spots were taken as a function of temperature. Temperatures higher than room temperature were attained by the use of a high temperature gas blower with which temperatures can be regulated within ±0.1 K. The superstructure spots disappeared between 150°C and 200°C above which the precession patterns correspond to the T* phase with P4/nmm symmetry. The transition from orthorhombic to tetragonal is still reversible after several heating and cooling cycles.

3.2. Four-circle diffractometer experiments

A single crystal platelet (0.32×0.32×0.04 mm^3) was mounted on a CAD4 diffractometer installed on a NONIUS FR 571 rotating anode generator operated at 57 kV and 60 mA. Graphite monochromatized AgKα radiation was used. High temperature cement was used to glue the crystal to the quartz fiber. The high temperatures were achieved by the same apparatus mentioned above, while for the low temperatures a modified Leybold nitrogen gas blower with a ±1°C temperature stability was used. The room temperature data collection was carried out first, then the temperature was gradually increased in 5 K steps up to 520 K. The cell parameters and several sub- and superstructure reflection profiles were measured at each temperature. At 520 K a second intensity data collection was carried out on the P4/nmm space group. Subsequently the temperature was decreased stepwise to room temperature and then to 150 K. The lattice parameters and reflection profiles were measured again at each temperature.

The room- and high temperature data collections were carried out using the ω-scan technique with a 1.4° scan width and 3 mm horizontal and vertical detector slits. The intensities of the reflections in-

cluded in the reciprocal sphere of radius $\theta = 30°$ were measured in both experiments, plus a half reciprocal sphere between 30° and 35° in θ for the room temperature experiment.

The cell parameters were obtained by refining the absolute θ values of 12 reflections with θ varying between 18° and 27°. The room temperature values are $a = b = 5.451(2)$ Å, $c = 12.426(6)$ Å. Their variation with temperature together with that of the unit cell volume is shown on fig. 2. They exhibit a Debye-like behavior without any transition in the temperature range investigated.

The intensity variation of some of the superstructure reflections is shown in fig. 3. They begin to exhibit a detectable intensity for $T < 470$ K, which increases slightly as the temperature is lowered to ≈ 380 K. By further lowering the temperature, the superstructure intensities increase strongly and begin to saturate at temperatures around 150 K. This means that the transition width is extremely large, at least 300 K. Thus, the room temperature intensity data, taken in the middle of the transition, would not yield the complete distortion of the structure. An intensity data collection at 50 K is in progress.

Sub- and superstructure reflection profiles are shown in fig. 4. A comparison between the profile of (410) superstructure reflection and that of (401) structure reflection shows that the superstructure reflection is broader. This indicates that the superstructure correlation length is finite and can be estimated at ≈ 300 Å. The same comparison (see fig. 5) at 273 K (after the high temperature data collection, i.e. after a heat treatment at 520 K for a few days) shows that both reflections (410) and (401) have become narrower, and the superstructure one has narrowed more than the structure reflection. This behavior can be better understood by following the evolution of the (410) superstructure profile from room temperature (before the high temperature data collection) to 273 K (after the high temperature data collection) to 173 K shown in fig. 6. It can be seen that the narrowing of the superstructure reflection takes place between room temperature and 273 K measurements. No additional effect is seen on further lowering of the temperature. It is reasonable to assume that the sharpening of the superstructure reflections is due to the sample annealing during the high temperature data collection. This conclusion is corroborated by the observation of the same effect, although much less pronounced, for the structure reflections.

3.3. Refinement of the tetragonal structure at 520 K

The intensities of 4354 reflections collected at 520 K were corrected for Lorentz-polarization effects and standard-reflection intensity variations. A Gaussian absorption correction in which the crystal shape is taken into account was applied. The reflections were averaged in the 4/mmm point group yielding 475 independent reflections with an internal consistency factor of 4.2%. This is a relatively high value, and is probably the result of discrepancies observed for the intensities of (hkl) and (khl) reflections. These discrepancies are due to the stress applied to the crystal because the thermal expansion of the cement, used to glue the sample to the quartz fiber, is larger than the thermal expansion of the crystal itself. A similar effect has been previously reported by Argoud and Muller [4]. In order to diminish it, an empirical correction was applied, after which a 2.6% value for the internal consistency factor was obtained.

The structural refinement was based on 406 reflections having $I > 3\sigma(I)$ and $\sin\theta/\lambda > 0.2$. The starting positional parameters were those of Izumi et al. for (Nd, Sr, Ce)$_2$CuO$_4$, with La in the 9-fold coordinated site and Tb in the 8-fold one. Low-angle reflections were excluded because, as checked by psi scan measurements, they were affected by multiple diffraction effects. During the final refinement cycles, the occupancy factors of La and Tb were varied and all atoms except O(2) had anisotropic thermal vibrations. The O2 atom had to be placed in the 8j (xxz) position because it exhibited an anomalously large thermal factor. This disorder was already observed for (Nd, Sr, Ce)$_2$CuO$_4$ by Izumi et al.. The final R-factors are $R = 3.5\%$ and $R = 3.4\%$, the occupancy factors of La and Tb are 1.034(1) and 0.966(1), respectively. If one assumes that the Pb cations are accommodated on the La site and that some of the Tb sites are occupied by La, the above values correspond to a chemical formula such as ($La_{0.599}$, $Tb_{0.362}$, $Pb_{0.039}$)$_2$CuO$_4$, which is in reasonable agreement with that determined by microana-

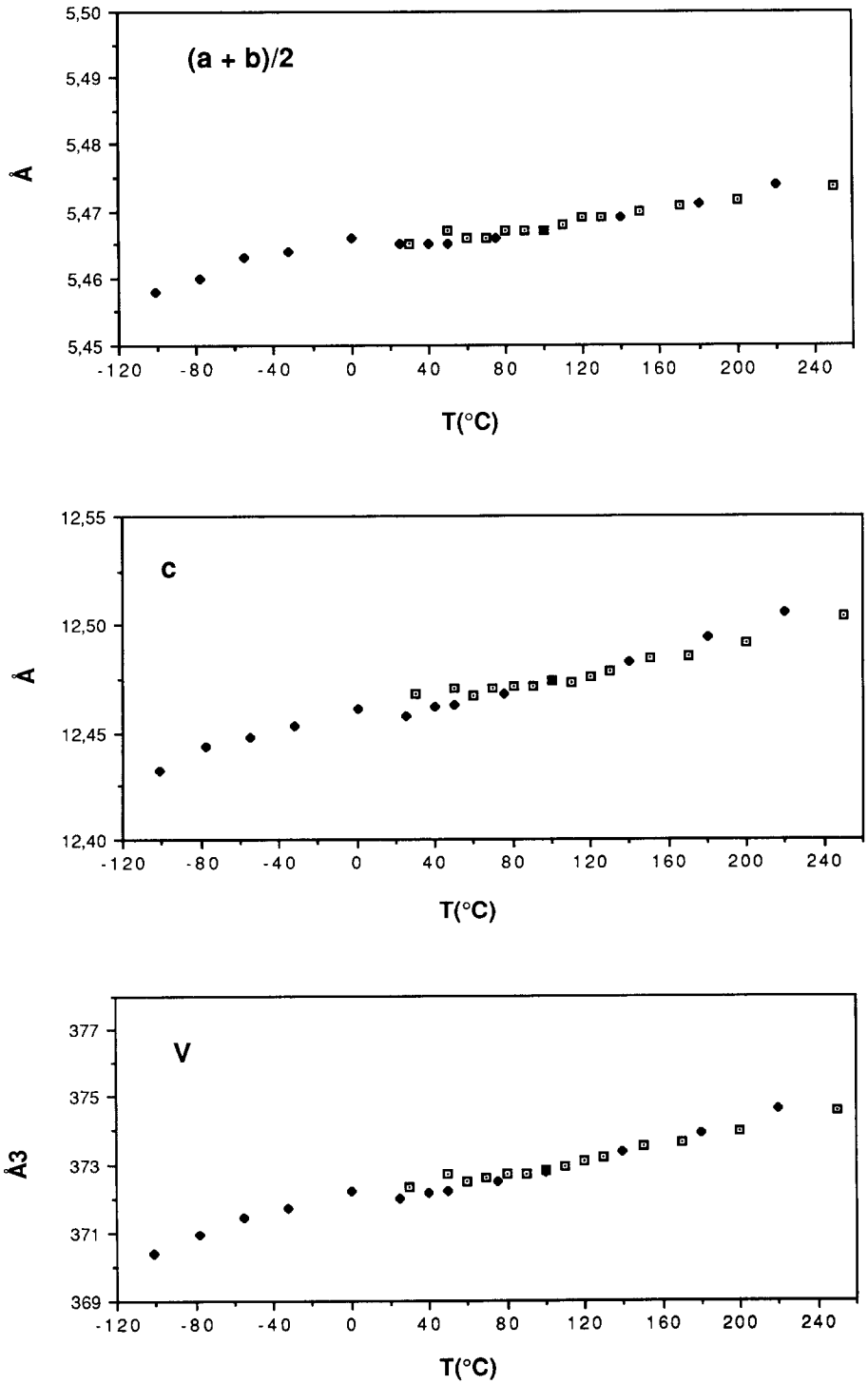

Fig. 2. Variation of the cell parameters and unit cell volume with temperature for (La, Tb, Pb)$_2$CuO$_4$. Since a and b were always found equal within one standard deviation, we have represented their average. Open symbols: increasing temperature; closed symbols: decreasing temperature.

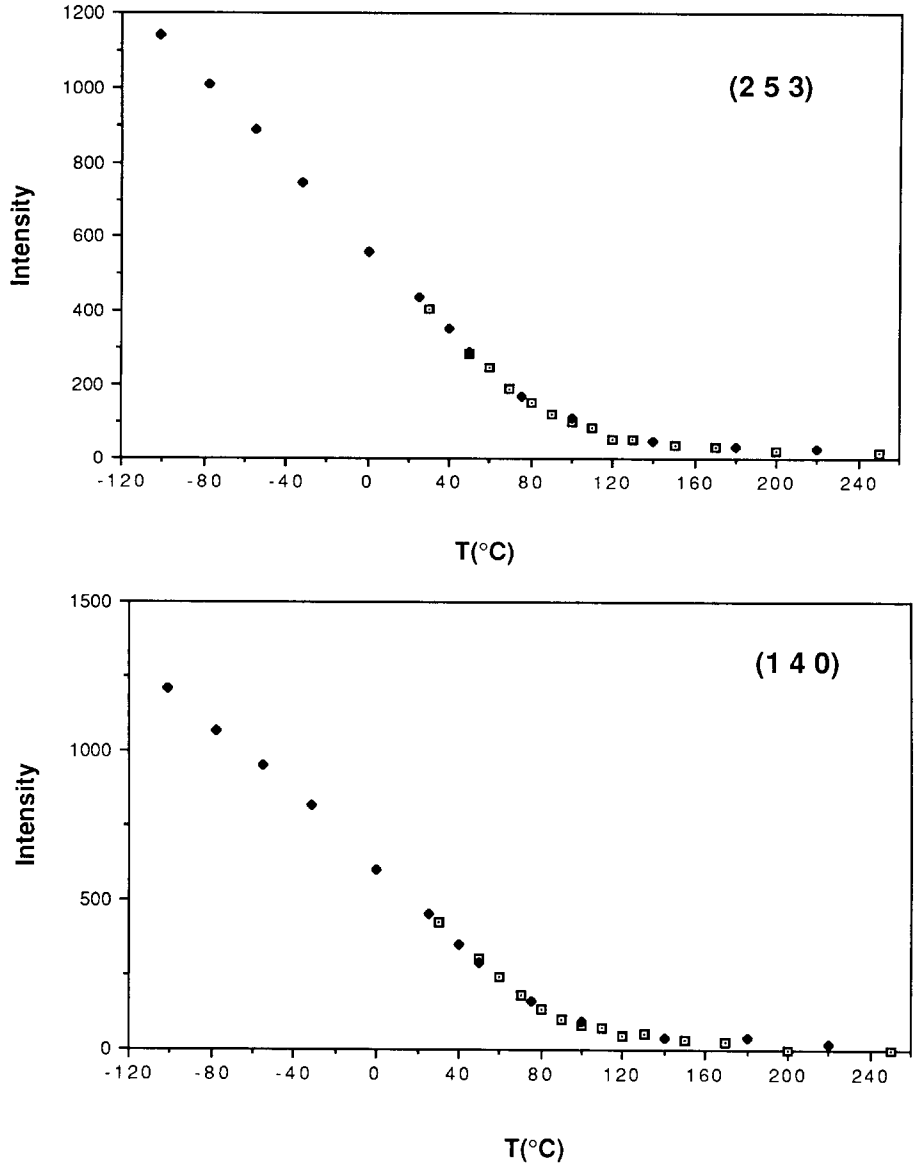

Fig. 3. Intensity variation of the (1 4 0) and (2 5 3) superstructure reflections as a function of temperature. Open symbols: increasing temperature; closed symbols: decreasing temperature.

lysis. The A sites are occupied by ($La_{0.92}$, $Pb_{0.08}$) whereas the A′ sites are occupied by ($Tb_{0.72}$, $La_{0.28}$). The crystallographic parameters and relevant interatomic distances are reported in table I. Attempts to refine the structure in orthorhombic Pmmn and monoclinic $P2_1$ (both subgroups of P4/nmm) with the data averaged before empirical corrections yielded insignificant deviation from the tetragonal symmetry.

4. Structural refinement of (La, Tb, Sr)$_2$CuO$_4$ by powder neutron diffraction

The powder neutron diffraction data were col-

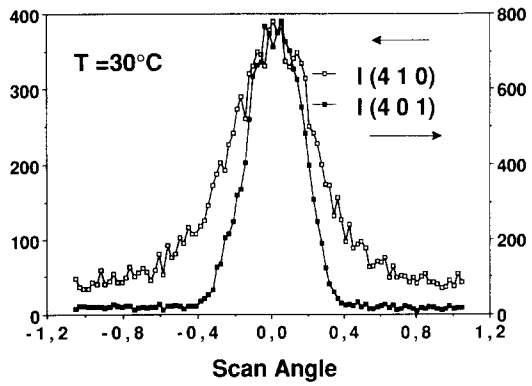

Fig. 4. The ω-scan profiles of the (4 1 0) superstructure reflection and the (4 0 1) structure reflection at room temperature (303 K).

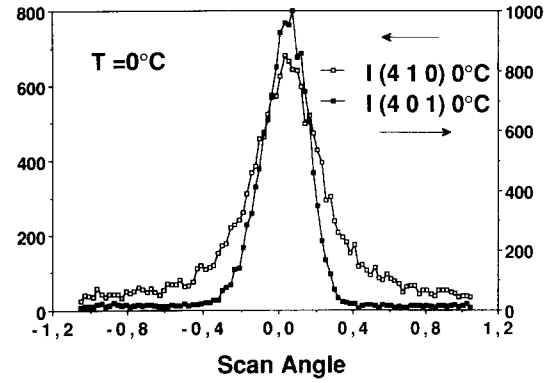

Fig. 5. Same as fig. 4, but the measurements are made at 273 K after the high temperature data collection.

lected at room temperature with the high resolution five-counter diffractometer at the Reactor of the National Institute of Standards and Technology. Neutrons of wavelength 1.553 Å were used in the experiment with in-pile, monochromatic beam, and diffracted beam collimators having horizontal angular divergencies of 10, 20 and 10 minutes of arc, respectively. The sample was placed in a vanadium can of about 1 cm in diameter and the data were collected in the angular range 5–120° in steps of 0.05°.

The structure was refined with the Rietveld method [5] adapted to five-detector geometry and modified to include background parameters [6]. The neutron scattering amplitudes used in the calculations were: $b(\mathrm{La})=0.827$, $b(\mathrm{Sr})=0.702$, $b(\mathrm{Tb})=0.738$,

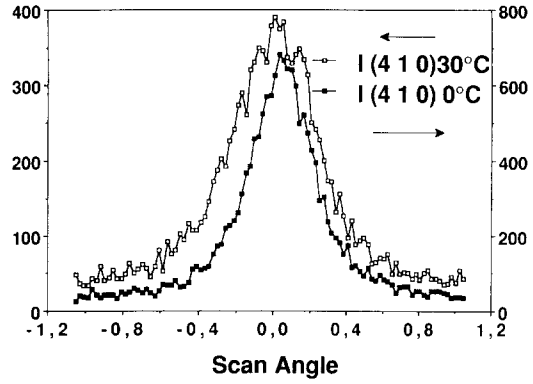

Fig. 6. Comparison of the ω-scan profiles of the (4 1 0) superstructure reflection measured at 303 K (empty squares) and 273 K (full squares) i.e. before and after the high temperature data collection, respectively.

$b(\mathrm{Cu})=0.772$ and $b(\mathrm{O})=0.581\times10^{-12}$ cm. The peak shapes could be described satisfactorily by Gaussian functions. The initial parameters were those of (Nd, Sr, Ce)$_2$CuO$_4$ [3]. As the nominal composition of the sample was (La$_{0.5}$, Tb$_{0.4}$, Sr$_{0.1}$)$_2$CuO$_4$ the refinements were started with (La$_{0.8}$, Sr$_{0.2}$) on the 9-coordinated site and (Tb$_{0.8}$, La$_{0.2}$) on the 8-coordinated one. Attempts to refine the relative occupancy factors of the cations for both sites did not modify the positional parameters and yielded unrealistic results for the composition of the 8-coordinated site. This is due to the small difference between the neutron scattering amplitudes for Tb and La cations and to the strong correlation between the occupancy and thermal factor of this site. Since the powder pattern did not contain reflections belonging to any impurity phases, the occupancy factors of the A and A′ sites were fixed at the nominal composition. As found for (Nd, Sr, Ce)$_2$CuO$_4$ and for (La, Tb, Pb)$_2$CuO$_4$, the O(2) atom had a large thermal factor indicating positional disorder. As for the previous cases, O(2) was placed in the less symmetrical position 8j (xxz). This resulted in a significant improvement of the R-factors. Attempts to refine the structure with O(2) placed in the general (xyz) position yielded unreasonable results and no improvement of the R-factors. The occupancy factors of the three oxygen sites were also varied. The refined values are 0.991(6), 0.500(3), 0.480(4) for O(1), O(2) and O(3), respectively. The occupancy

Table I
Positional and thermal parameters for (La, Tb, Pb)$_2$CuO$_4$ at 520 K.

Atom	Position	Occup.	x	y	z	U_{11}	U_{22}	U_{33}
La	2c	1.034(1)	1/4	1/4	0.38436(3)	0.01457(8)	0.01457(8)	0.0133(1)
Tb	2c	0.966(1)	1/4	1/4	0.09683(3)	0.00885(6)	0.00885(6)	0.0133(1)
Cu	2c	1	1/4	1/4	0.75594(7)	0.0061(2)	0.0061(2)	0.0180(3)
O(1)	4f	1	3/4	1/4	0.2378(3)	0.024(3)	0.003(2)	0.035(2)
O(2)	8j	1	0.295(1)	0.295(1)	0.5716(5)	1.1(1)		
O(3)	2a	1	3/4	1/4	0	0.011(1)	0.011(1)	0.023(2)

$a=b=3.870(2)$ Å, $c=12.504(6)$ Å

La–O(1)×4	2.665(3)	Tb–O(1)×4	2.618(3)
La–O(2)×1	2.354(6) (apical)	Tb–O(3)×4	2.283(2)
×2	2.802(4)	Cu–O(1)×4	1.937(2)
×1	2.553(4)	Cu–O(2)×1	2.318(6)
×1	3.031(4)		

Table II
Positional and thermal parameters for (La, Tb, Sr)$_2$CuO$_4$ at room temperature.

Atom	Position	Occup.	x	y	z	B
La	2c	0.8La/0.2Sr	1/4	1/4	0.3849(1)	0.75(3)
Tb	2c	0.8Tb/0.2La	1/4	1/4	0.0996(1)	0.45(4)
Cu	2c	1	1/4	1/4	0.7549(1)	0.57(3)
O1	4f	0.991(6)	3/4	1/4	0.2358(2)	1.35(4)
O2	8j	1.000(6)	0.2959(9)	0.2959(9)	0.5733(2)	0.73(5)
O3	2a	0.960(8)	3/4	1/4	0	1.59(6)

$a=b=3.8510(1)$ Å, $c=12.5039(2)$ Å

La–O(1)×4	2.6808(2)	Tb–O(1)×4	2.5699(2)
La–O(2)×1	2.369(10) (apical)	Tb–O(3)×4	2.2934(9)
×2	2.784(2)	Cu–O(1)×4	1.9291(3)
×1	2.528(2)	Cu–O(2)×1	2.284(5)
×1	3.019(3)		

factor of O(3) is within 5 times the standard deviation from full and its value could be significant. Recently, Kwei et al. [7] refined the structure of (La$_{0.45}$, Sm$_{0.45}$Sr$_{0.10}$)$_2$CuO$_4$ from powder neutron diffraction data and, in agreement with our results, found that the O(2) and O(3) sites are fully and partially occupied, respectively. However, the occupancy factor for (La$_{0.45}$, Sm$_{0.45}$Sr$_{0.10}$)$_2$CuO$_4$ is substantially smaller (0.869(7)) than the value we determined for (La$_{0.5}$, Tb$_{0.4}$Sr$_{0.2}$)$_2$CuO$_4$ (0.960(8)). In view of these results and those of Izumi et al. [3] who found that the O(3) sites are fully occupied and the O(2) ones are oxygen deficient, we feel that the departure from the O$_4$ stoichiometry and which would be the deficient sites, are still open questions.

5. Discussion

Except for the oxygen stoichiometry, the structural results for (La, Tb, Pb)$_2$CuO$_4$ and (La, Tb, Sr)$_2$CuO$_4$ are very similar to those obtained by Izumi et al. for (Nd, Sr, Ce)$_2$CuO$_4$. The positional parameters and the interatomic distances for the three structures are reported in table III(a) and III(b). Note that the displacement of the O(2) atom is the same for three structures within one standard deviation. The most

Table III (a)
Comparison of the positional parameters (a) and interatomic distances (b) obtained for the T* phase compounds (La, Tb, Pb)$_2$CuO$_4$ (1, this work), (La, Tb, Sr)$_2$CuO$_4$ (2, this work) and (Nd, Sr, Ce)$_2$CuO$_4$ (3, Izumi et al. [3]).

Atom	Position	Occup.	x	y	z
A (1)		0.92La/0.08Pb			0.38436(3)
A (2)	2c	0.8La/0.2Sr	$\frac{1}{4}$	$\frac{1}{4}$	0.3849(1)
A (3)		0.59Nd/0.41Sr			0.3893(3)
A′ (1)		0.72Tb/0.28La			0.09683(3)
A′(2)	2c	0.8Tb/0.2La	$\frac{1}{4}$	$\frac{1}{4}$	0.0996(1)
A′(3)		0.73Nd/0.27Ce			0.1035(3)
Cu (1)					0.75594(7)
Cu (2)	2c	1	$\frac{1}{4}$	$\frac{1}{4}$	0.7549(1)
Cu (3)					0.7490(3)
O(1) (1)		1			0.2378(3)
O(1) (2)	4f	0.991(6)	$\frac{3}{4}$	$\frac{1}{4}$	0.2358(2)
O(1) (3)		1			0.2378(3)
O(2) (1)		1	0.295(1)	0.295(1)	0.5716(5)
O(2) (2)	8j	1.000(6)	0.2959(9)	0.2959(9)	0.5733(2)
O(2) (3)		0.92(2)	0.296(6)	0.296(6)	0.5709(6)
O(3) (1)		1			
O(3) (2)	2a	0.960(8)	$\frac{3}{4}$	$\frac{1}{4}$	0
O(3) (3)		1			

Table III (b)

Distance	(La, Tb, Pb)$_2$CuO$_4$	(La, Tb, Sr)$_2$CuO$_4$	(Nd, Sr, Ce)$_2$CuO$_4$
A –O(1)×4	2.665(3)	2.6808(2)	2.701(3)
A –O(2)×1	2.354(6)	2.369(10)	2.281(9)
A –O(2)×2	2.802(4)	2.784(2)	2.783(3)
A –O(2)×1	2.553(4)	2.528(2)	2.53(3)
A –O(2)×1	3.031(4)	3.019(3)	3.02(3)
A′–O(1)×4	2.618(3)	2.5699(2)	2.555(3)
A′–O(3)×4	2.283(2)	2.2934(9)	2.321(2)
B –O(1)×4	1.937(2)	1.9291(3)	1.9352(4)
B –O(2)×1	2.318(6)	2.284(5)	2.238(9)

puzzling question concerning the structure of the T* phase is the origin of the positional disorder observed for the O(2) atom in the three compounds. Izumi et al. attributed it to a partial ordering between the Nd and Sr cations on the 9-coordinated site. However, since the differences in size of the cations occupying this site vary substantially from one compound to the other, while the oxygen displacement remain exactly the same, the cation ordering cannot be the cause of this displacement. Moreover, the phase transition observed for (La, Tb, Pb)$_2$CuO$_4$ cannot be interpreted in terms of cation ordering of cations since movements of such large cations are very unlikely to occur in the temperature range where the transition is observed.

It seems reasonable then to assume that the O(2) displacement is intrinsic to the T* structure and is related to the superstructure observed in (La, Tb, Pb)$_2$CuO$_4$ below 470 K. This superstructure is due to ordered canting of the CuO_5 pyramids, and the displacement of the O(2) atom at temperatures above the transition indicates a disordered canting of these pyramids.

The canting of the pyramidal axis in the T* structure could be related to the octahedral tilting which occurs at the tetragonal to orthorhombic transition

observed in the T phase of $La_{2-x}M_xCuO_4$ (M=Ba, Sr, etc...). In the orthorhombic structure of the latter system the octahedra tilt as rigid units, that is, the apices follow the buckling of the basal plane. In the tetragonal structure of the T* phases the disordered canting does not involve the buckling of the pyramidal base, however, it is possible that in the orthorhombic structure of the T* phases the canting, besides becoming ordered, would involve the entire pyramid and not only its apex.

In $La_{2-x}M_xCuO_4$(M=Ba, Sr, etc...) the transition temperature is a function of x and of the nature of the M cation. A structural transition similar to that observed for (La, Tb, Pb)$_2$CuO$_4$ should occur in all the T* compounds at some given temperature. Recently, some superstructure reflections have been detected by electron diffraction on a ($La_{1.0}$, $Sm_{0.8}$, $Sr_{0.2}$)CuO_4 sample at liquid nitrogen temperature.

The A′ sites are also occupied by two different types of cations, however, no ordering is detected as the two types of oxygen atoms forming the 8-fold coordination polyhedra of the A′ cations (O(1) and O(3)) have normal temperature factors in the three structures. The average A′–O distances for (La, Tb, Pb)$_2$CuO$_4$, (La, Tb, Sr)$_2$CuO$_4$ and (Nd, Sr, Ce)$_2$CuO$_4$ are: 2.451(0.179) Å, 2.432(0.148) Å and 2.438(0.125) Å, respectively. The number between parentheses represent the standard deviations of the average distance calculated as if the individual distances were independent measurements. Such a value gives an estimate of the polyhedron distortion. These distances are in good agreement with the average ionic radii calculated from the values tabulated by Shannon [8] for 8-coordinated cations (2.454 Å, 2.444 Å and 2.451 Å, respectively).

The A′ cation sizes decrease on going from (La, Tb, Pb)$_2$CuO$_4$ to (La, Tb, Sr)$_2$CuO$_4$, while the individual distances, A′–O(1) and A′–O(3), decrease and increase, respectively. The decrease of the A′–O(1) distances is due to two factors, one is the size decrease of the A′ cation and the other is the size increase of the A cation. Four O(1) atoms are shared between the two polyhedra around the A′ and the A cations. As the latter increases in size on going from (La, Tb, Pb)$_2$CuO$_4$ to (La, Tb, Sr)$_2$CuO$_4$, the A–O(1) distances increase resulting in a shift of the O(1) atoms towards the A′ cations. This additional decrease of the A′–O(1) distances is compensated by an increase of the A′–O(3) distances, which increase while A′ decreases. The same does not seem to be valid for (Nd, Sr, Ce)$_2$CuO$_4$, which is probably due to the presence of the tetravalent Ce^{4+} on the A′ sites. In order to have electrostatic equilibrium the distortion of the A′ sites must depend upon the cation charge.

The Cu cations occupy pyramidal sites with four short bonds (Cu–O(1)$\approx$1.93 Å) and one longer bond. The main difference between the three structures concerns the longer Cu–O(2) distances, which varies from 2.318 Å in (La, Tb, Pb)$_2$CuO$_4$ to 2.238 Å in (Nd, Sr, Ce)$_2$CuO$_4$. This distance to the apical oxygen of the Cu coordination pyramid has been shown to be crucial for the superconducting properties of the high-T_c cuprate superconductors [9]. For instance, in the $YBa_2Cu_3O_{6+x}$ series, the apical oxygen distance decreases as x and T_c increase. This variation corresponds to a charge transfer from the chain copper cations to the plane ones. In the present case, the apical oxygen distance is 0.05 Å shorter for (Nd, Sr, Ce)$_2$CuO$_4$ which is superconducting, than for the other two compounds, which are not superconducting. Thus, the same kind of mechanism can be invoked here, i.e. the positive charges created by the substitution of Nd^{3+} by Sr^{2+} are transferred to the CuO_2 plane via the shortening of the apical oxygen distance. It must be pointed out, though, that this model does not explain why the deoxidized sample of (Nd, Sr, Ce)$_2$CuO$_4$ reported by Izumi et al. is nonsuperconducting. The apical oxygen–planar Cu distance in this sample is exactly the same as that of the oxidized superconducting sample.

The valence of the Cu cations can be calculated by using the Zachariasen bond length–bond strength relation [10]. We use the constants A=0.171 and D1=1.724 determined from the $YBa_2Cu_3O_6$ structure [11]. We find 2.075^+, 2.145^+ and 2.130^+ for the valences of the Cu cations in the (La, Tb, Pb)$_2$CuO$_4$, (La, Tb, Sr)$_2$CuO$_4$ and (Nd, Sr, Ce)$_2$CuO$_4$ structures, respectively. This is in good agreement with the values (2.08^+, 2.20^+ and 2.14^+, respectively) obtained by assuming electrical neutrality and the normal valences for the A and A′ cations. Note that the Cu valence is higher for nonsuperconducting (La, Tb, Sr)$_2$CuO$_4$ than for superconducting (Nd, Sr, Ce)$_2$CuO$_4$. This is due to the small value of the a parameter for (La, Tb,

Sr)$_2$CuO$_4$ which compensates the longer apical distance. The distances reported by Izumi et al. for their nonsuperconducting deoxidized sample lead to a 2.140^+ valence for Cu which is even higher than the one reported above for the oxidized sample.

Acknowledgement

The authors wish to thank Catherine Chaillout for performing the low temperature electron diffraction experiment on the ($La_{1.0}$ $Sm_{0.8}$ $Sr_{0.2}$)CuO_4 sample.

References

[1] E. Takayama-Muromachi, Y. Matsui, Y. Uchida, F. Izumi, M. Onoda and K. Kato, Jpn. J. Appl. Phys. 27 (1988) L2283.

[2] J. Akimitsu, S. Susuki, M. Watanabe and H. Sawa, Jpn. J. Appl. Phys. 27 (1988) L1859.

[3] F. Izumi, E. Takayama-Muromachi, A. Fujimori, T. Kamiyama, H. Asano, J. Akimitsu and H. Sawa, Physica C 158 (1989) 440.

[4] R. Argoud and J. Muller, J. Appl. Crystallogr., 22 (1989) 378.

[5] H.M. Rietveld, J. Appl. Crystallogr., 2 (1969) 65.

[6] E. Prince, Natl. Bur. Stand. US Tech. Note no. 1117 (1980) p. 8.

[7] G.H. Kwei, R.B. Van Dreele, S-W. Cheong, Z. Fisk, J.D. Thompson and J.E. Shirber, preprint.

[8] R.D. Shannon, Acta Crystallogr. A 32 (1976) 751.

[9] R.J. Cava, A.W. Hewat, E.A. Hewat, B. Batlogg, M. Marezio, K.M. Rabe, J.J. Krajewski, W.F. Peck Jr. and L.W. Rupp Jr., Physica C 165 (1990) 419.

[10] W.H. Zachariasen, J. Less-Common Met. 62 (1978) 1.

[11] P. Bordet, Thèse d'Etat, Grenoble (1989).